Electronic Supplementary Material (ESI) for Reaction Chemistry & Engineering.


# Supporting Information

## The effects of dimensionality of tin oxide-derived catalysts on $CO_2$ reduction by using gas-diffusion electrodes

Mengran Li[1], Mohamed Nazmi Idros[1], Yuming Wu[1], Sahil Garg[1], Shuai Gao[1], Rijia Lin[1], Hesamoddin Rabiee[2], Zhiheng Li[1], Lei Ge[1,3,*], Thomas Edward Rufford[1,*], Zhonghua Zhu[1], Liye Li[4], Geoff Wang[1]

1. School of Chemical Engineering, the University of Queensland, St Lucia, 4072, Brisbane, Queensland, Australia
2. Advanced Water Management Centre, Faculty of Engineering, Architecture and Information Technology, The University of Queensland, St. Lucia, Queensland 4072, Australia
3. Centre for Future Materials, University of Southern Queensland, Springfield Central, Queensland 4300, Australia
4. HBIS Group Technology Research Institute, Shijiazhuang, 050023, China
Corresponding authors:

L. Ge: lei.ge@usq.edu.au; T. Rufford: t.rufford@uq.edu.au

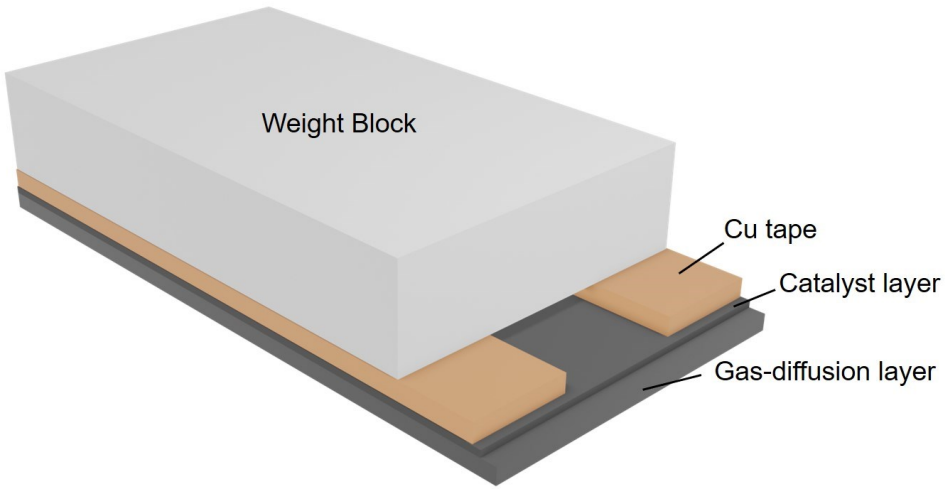


Figure S 1 Custom-made apparatus to measure surface electrical resistance of the catalyst layer of the gas-diffusion electrodes. The weight block is to ensure the same pressure applied to the catalyst layers. The copper tapes are used to conduct electricity and are connected with the potentiostat for linear scanning voltammetry analysis. One working electrode and sensor probe of the potentiostat are connected with one tape, and counter & reference electrode probe of the potentiostat are connected to the other tape. This configuration minimizes the resistance contributed from the cable between the connection point and potentiostat. The copper tapes are adhered to the weight block with fixed dimensions for each measurement. The electrode was cut to the same size for the measurement. This measurement assumes that the carbon substrate and the copper tape are significantly more conductive than the SnOx-based catalyst layer, so that the resistance is mainly contributed by the catalyst layer.

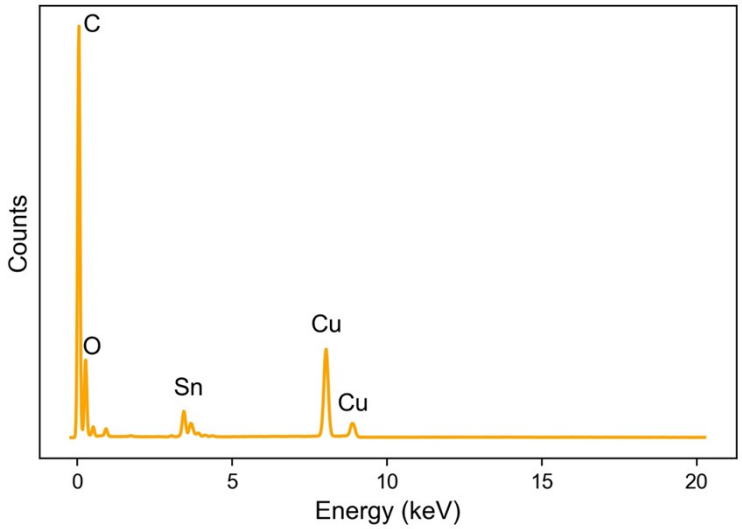


Figure S 2 EDS spectrum of the SnOx ns.

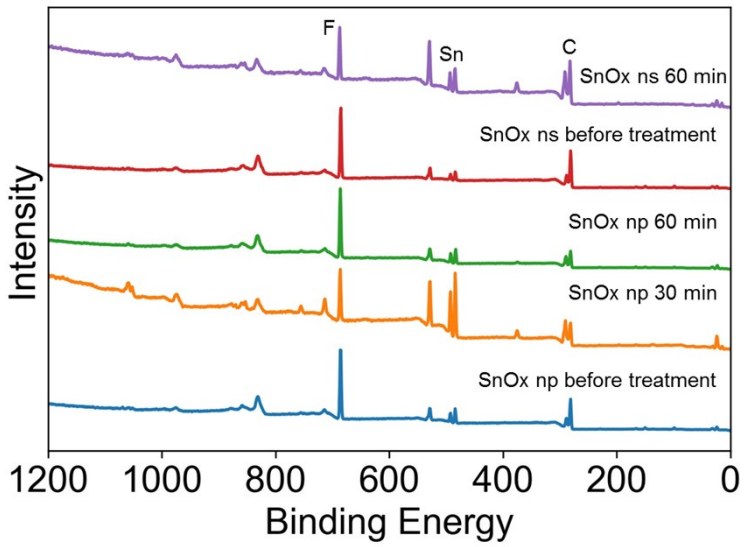


Figure S 3 XPS general survey of the SnOx np and SnOx ns at the catalyst layer of the GDEs before and after $CO_2$ electrochemical reduction treatment at 150 mA $cm^{-2}$.

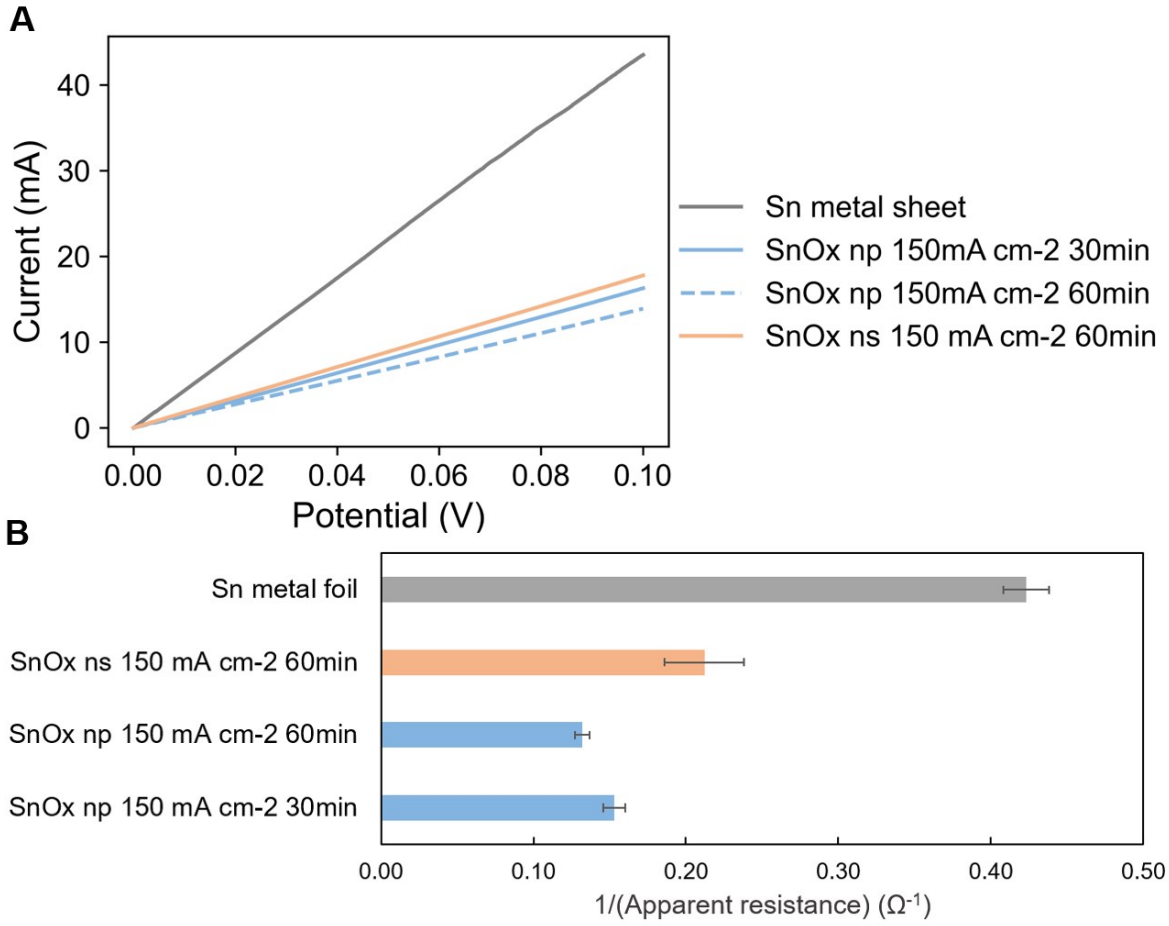


Figure S 4 (A) A comparison of the linear scanning voltammetry results and (B) apparent surface conductivities of Sn metal foil, and SnOx ns and SnOx np after electrochemical treatment at 150 mA $cm^{-2}$.

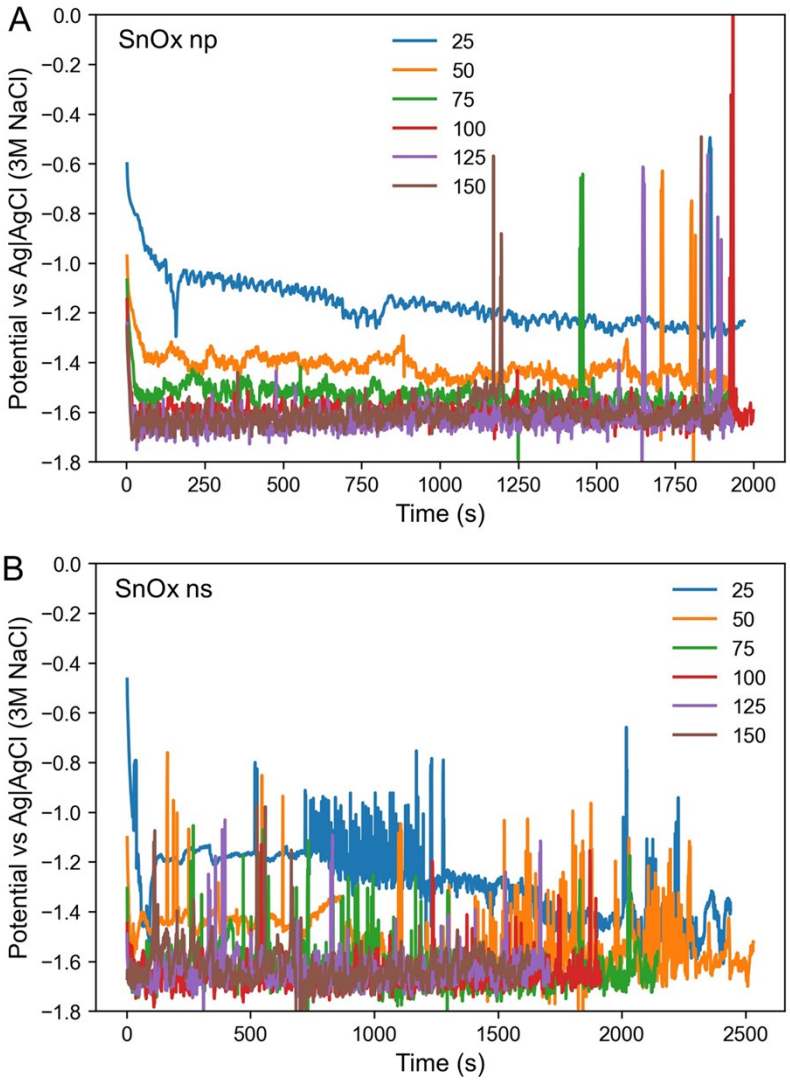


Figure S 5 Potential measured versus Ag|AgCl (3M NaCl) for varied current density over (A) SnOx np and (B) SnOx ns.

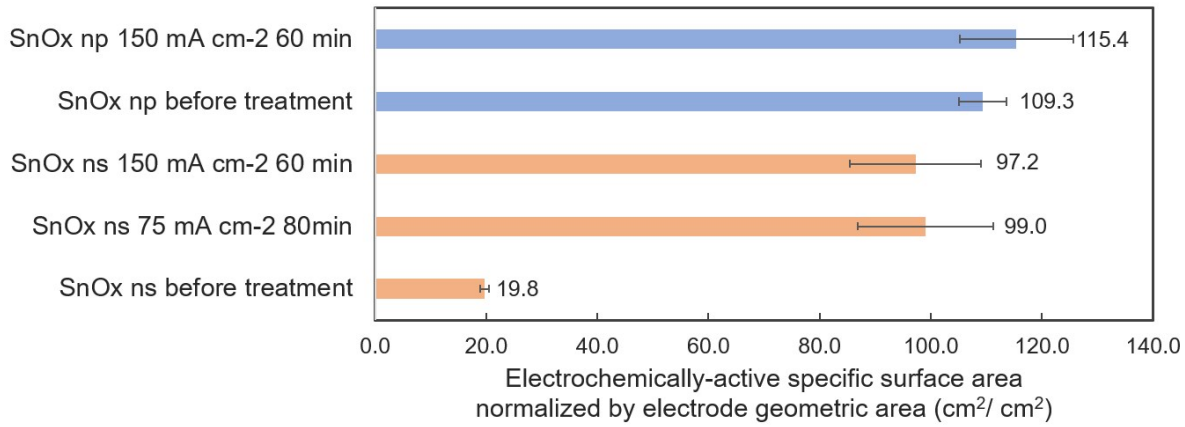


Figure S 6 Specific electrochemically-active surface area of the SnOx np and SnOx ns catalyst layer before and after $CO_2$ electrochemical reduction.

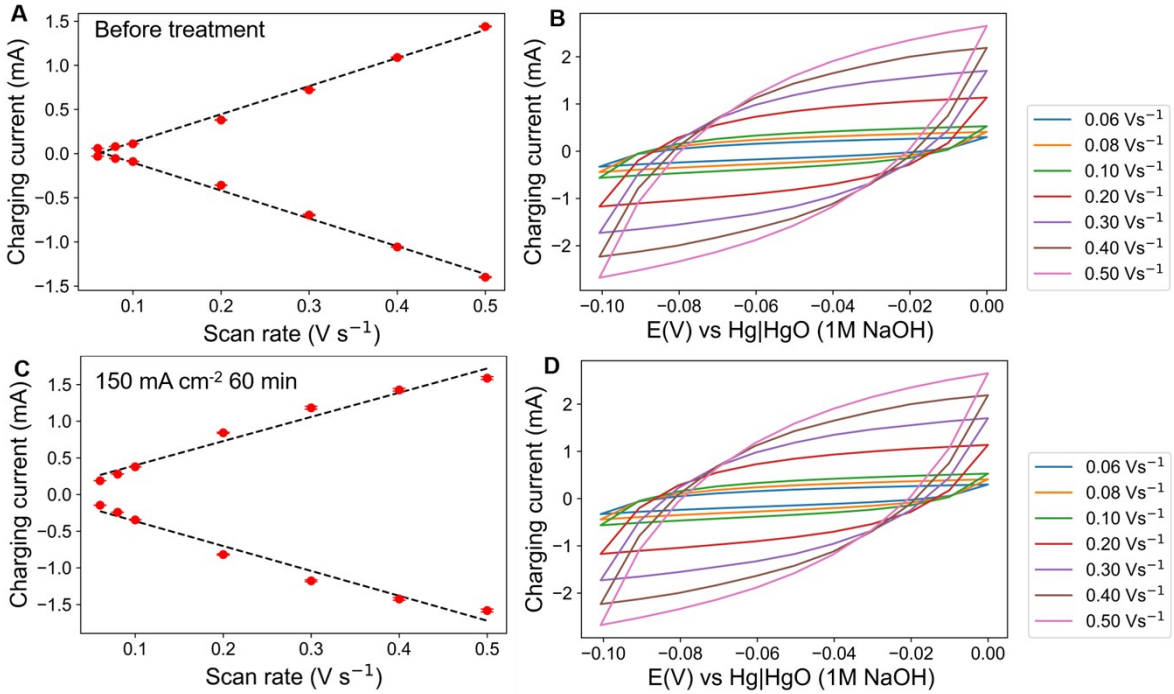


Figure S 7 (A) The capacitive current vs. scan rate and (B) charging current as a function of the potentials over SnOx np-based GDE of a geometric area of 1.8 $cm^2$. (C) The capacitive current vs. scan rate and (D) charging current as a function of the potentials over SnOx np-based GDE of a geometric area of 1.76 $cm^2$ after being treated at 150 mA $cm^{-2}$ for 60 min in a flow cell. The experiment is conducted in 0.5 M $KHCO_3$ in an H-cell. The treated electrodes were cut into a small size to fit the H-cell setup.

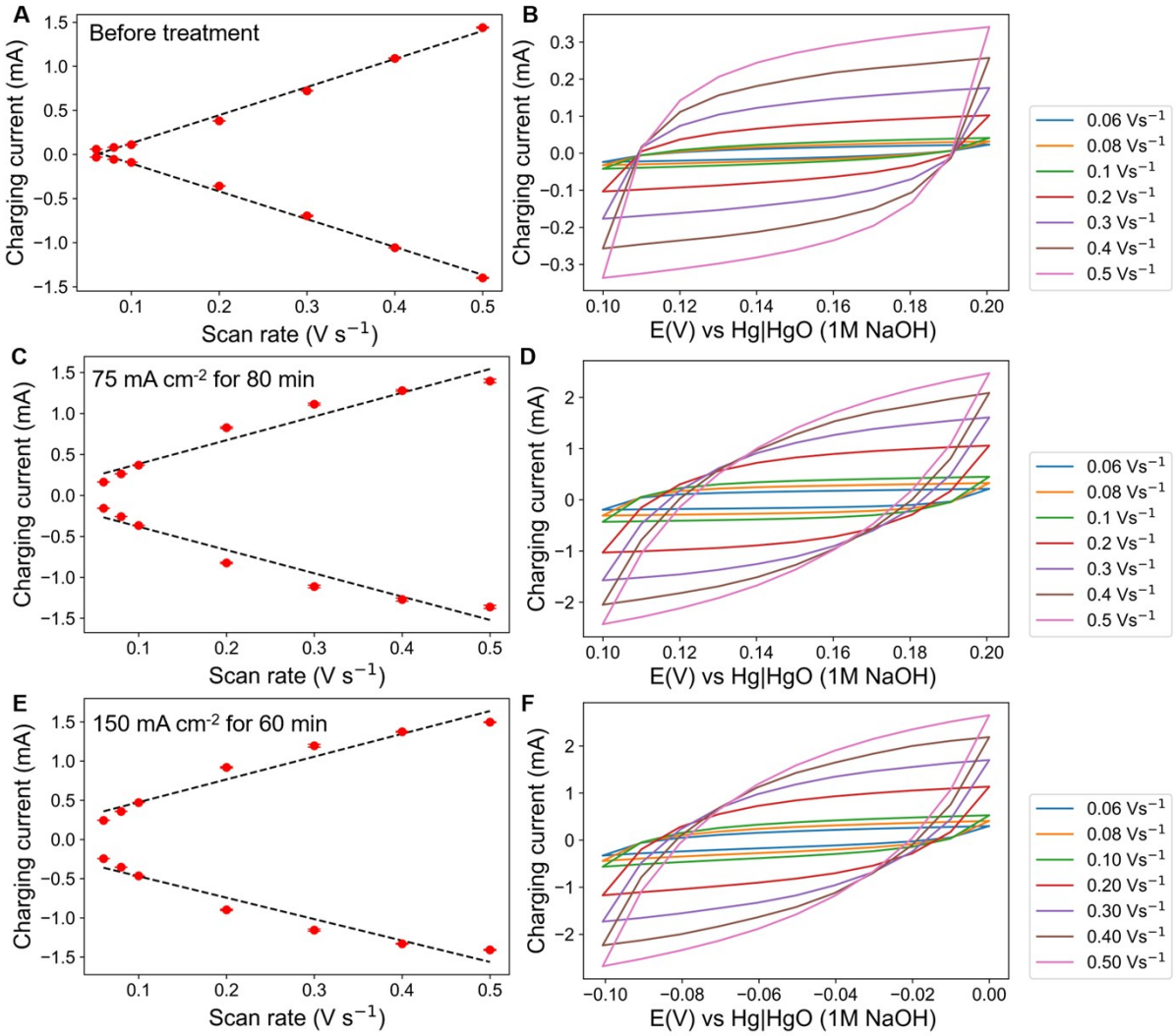


Figure S 8 The capacitive current vs. scan rate and charging current as a function of the potentials over SnOx ns-based GDE of a geometric area of 1.8 $cm^2$ before and after $CO_2$ electrochemical test in a flow cell. The experiment is conducted in 0.5 M $KHCO_3$ in an H-cell. The treated electrodes were cut into a small size to fit the H-cell setup.

Table S1 Comparison of $CO_2R$ catalytic performance of GDEs with SnOx np and SnOx ns as catalyst with other tin oxide-derived catalysts reported recently on GDEs.

| Catalyst | Loading, mg $cm^{-2}$ | Electrolyte | Potential, V vs RHE | FE ($HCOO^-$), % | j ($HCOO^-$), mA $cm^{-2}$ | Reference |
|---|---|---|---|---|---|---|
| **SnOx np** | 0.5 | 0.5 M $KHCO_3$ | -0.99 | 81 | 81 | This work |
| **SnOx ns** | 0.5 | 0.5 M $KHCO_3$ | -1.03 | 77 | 116 | This work |
| **nanorod@2D SnO nanosheet** | 1 | 1M KOH | -0.8 | 87 | 383 | Ref. (1) |
| **$SnO_2$ nanoparticles** | 0.35 | 0.5 M $Na_2SO_4$ + 0.5M $Na_2CO_3$ | -0.93 | 70 | 385 | Ref. (2) |
| **$SnO_2$ 5 nm** | 1.5 | 1 M $KHCO_3$ | -0.95 | 64 | 117 | Ref. (3) |
| **$SnO_2$ 10-15 nm** | 0.75 | 0.45 M $KHCO_3$ + 0.5 M KCl | -1.5[a] | 70 | 105 | Ref. (4) |
| **$SnO_2$ <100 nm** | 0.75 | 0.4 M $K_2SO_4$ | NA | 90 | 450 | Ref. (5) |

*a denotes that the potential reported is not referenced to RHE.*

## References


1. Qian Y, Liu Y, Tang H, Lin B-L, *J. CO2 Util.*, 2020,**42**,101287.
2. Sen S, Brown SM, Leonard M, Brushett FR, *J. Appl. Electrochem.*, 2019,**49**,917-28.
3. Liang C, Kim B, Yang S, Yang L, Francisco Woellner C, Li Z, Vajtai R, Yang W, Wu J, Kenis PJA, Ajayan Pulickel M, *J. Mater. Chem. A*, 2018,**6**,10313-9.
4. Del Castillo A, Alvarez-Guerra M, Solla-Gullón J, Sáez A, Montiel V, Irabien A, *J. CO2 Util.*, 2017,**18**,222-8.
5. Chen Y, Vise A, Klein WE, Cetinbas FC, Myers DJ, Smith WA, Deutsch TG, Neyerlin KC, *ACS Energy Lett.*, 2020,**5**,1825-33.